SUPPORTING INFORMATION: Polaritonic Chemistry: Collective Strong Coupling Implies Strong Local Modification of Chemical Properties

Dominik Sidler,[*,†,‡] Christian Schaefer,[*,†,‡] Michael Ruggenthaler,[*,†,‡] and Angel Rubio[*,†,‡,¶]

†*Max Planck Institute for the Structure and Dynamics of Matter and Center for Free-Electron Laser Science, Luruper Chaussee 149, 22761 Hamburg, Germany*

‡*The Hamburg Center for Ultrafast Imaging, Luruper Chaussee 149, 22761 Hamburg, Germany*

¶*Center for Computational Quantum Physics, Flatiron Institute, 162 5th Avenue, New York, NY 10010, USA*

E-mail: dsidler@mpsd.mpg.de; christian.schaefer@mpsd.mpg.de; michael.ruggenthaler@mpsd.mpg.de; angel.rubio@mpsd.mpg.de

Method

QEDFT and DFT simulations were performed with OCTOPUS[1] using the light-matter linear response framework for cavities, which was introduced in Ref. 2. For the ground state calculation, the optimized effective potential method with Krieger-Li-Iafrate (KLI) approximation[3–5] was employed. Perturbations of the groundstate density due to the photon field were not considered for consistency with usual quantum optics model assumptions.

Each individual nitrogen dimer was aligned along the y-axis, whereas the chain extends along the x-axis with a cavity coupled along the z-axis (other cavity orientations are discussed in the SI). The dimers were separated 1.32 nm with respect to their nearest neighbors in order to mimic (quasi) independent subsystems, which are mainly coupled via the cavity mode (dilute gas limit). This clearly avoids any density overlap in the chosen energy range of interest without the presence of a cavity. Simulations were performed for $N \in \{1, .., 8\}$ with $N - 1$ unperturbed dimers and a single perturbed dimer, which is always located at the center of the chain. The geometry of the ground-state nitrogen dimers was minimized in OCTOPUS reaching a nuclei distance of 107.9 pm, for the unperturbed dimers. The nuclear distance of the perturbed dimer was set to 110.5 pm, which shifts the lowest lying excitation in the absorption spectrum from $\hbar\omega_u = 13.309$ eV for the unperturbed dimer to $\hbar\omega_p = 13.206$ eV for an uncoupled system (i.e. for $\lambda = 0$). Core electrons of the nitrogen atoms were approximated with the standard Troullier-Martins pseudopotential, included in the OCTOPUS distribution. A real space Cartesian mesh with 15.9 pm grid spacing was used for the wave-function representation with minimum boxshape radius 1.06 nm. For derivative calculations, the standard OCTOPUS fourth order star stencils scheme was applied.

During the groundstate calculation, additional 120 unoccupied extrastates were minimized in the SCF cycles, which are necessary to extract the excited states in the linear response framework. One cavity mode was considered in the calculations. It was tuned to the calculated resonance frequency $\omega_c = \omega_u$, which corresponds to the first excitation of the unperturbed nitrogen dimer in the absence of a cavity. To give access to the three different

scaling regimes {I,II,III}, three different cavity coupling parameters were considered, which were set by $\lambda \in \{\frac{2}{3}, 1, 2\} \times 0.005$. Additional simulations were conducted in regime II with a (de)-tuned cavity on resonance with the perturbed dimer, i.e. $\omega_c = \omega_p$ (see SI). Local observables (e.g. dipole transition moments, transition densities) were extracted from the spatially resolved output of the diagonal elements of the transition density matrix,[6] using a customized python script. The oscillator strenghts were Lorentz broadened with a full width at half maximum of 5.4 meV to derive the spectral strength function. For illustration purposes, locally resolved transition densities were projected onto the z-axis, i.e. in agreement with the chosen cavity orientation $\boldsymbol{\lambda} \parallel \mathbf{e}_z$. Moreover, only significant transition densities are displayed with a magnitude larger than ± 0.005 for the individually resolved dimers and for the dark states. In contrast, to clear the data, the transition densities with respect to N were integrated over the energy windows, which can be attributed to the lower, middle and upper polaritonic branches respectively. Analyses showed little differences compared with solely considering the respective main contributors, except in the vicinity of the observed splitting of the upper polaritonic branch for $N = 7$ with $\lambda = 0.005$, which will be subject of future investigations.

Simulation Results for Coupling Regime I ($\lambda = 0.0033$)

Absorption Spectra for Cavity in Resonance with Unperturbed Dimers

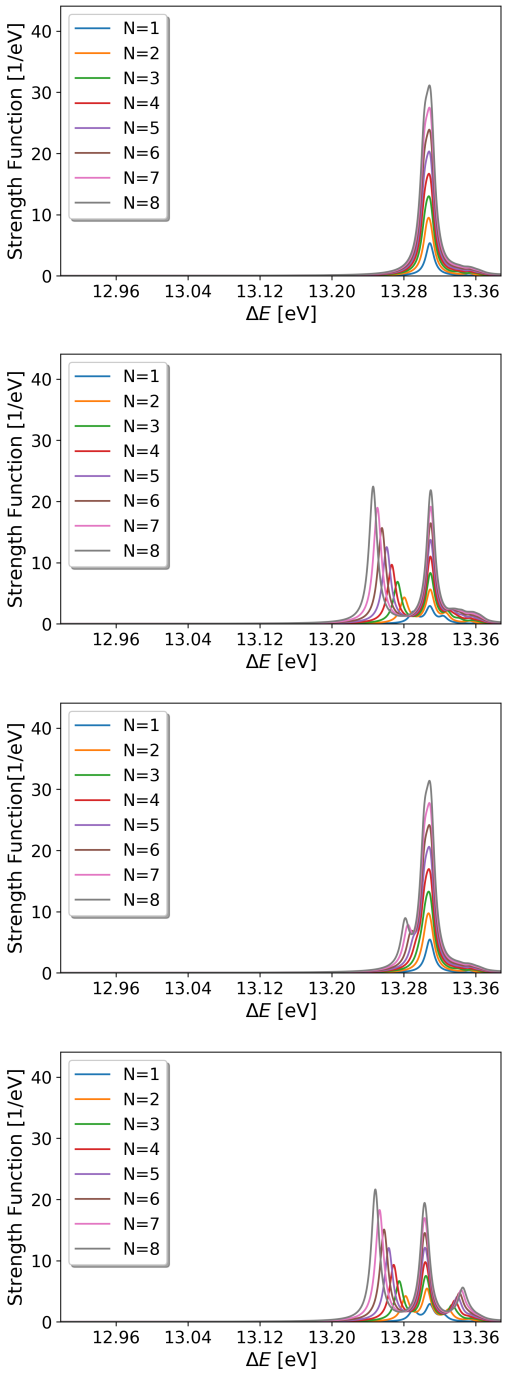

Figure S1: Nitrogen dimer chain of variable size $N \in \{1..9\}$ without perturbed dimer. From top to bottom: $\boldsymbol{\lambda} = 0$, $\boldsymbol{\lambda} \parallel \mathbf{e}_x$, $\boldsymbol{\lambda} \parallel \mathbf{e}_y$ and $\boldsymbol{\lambda} \parallel \mathbf{e}_z$.

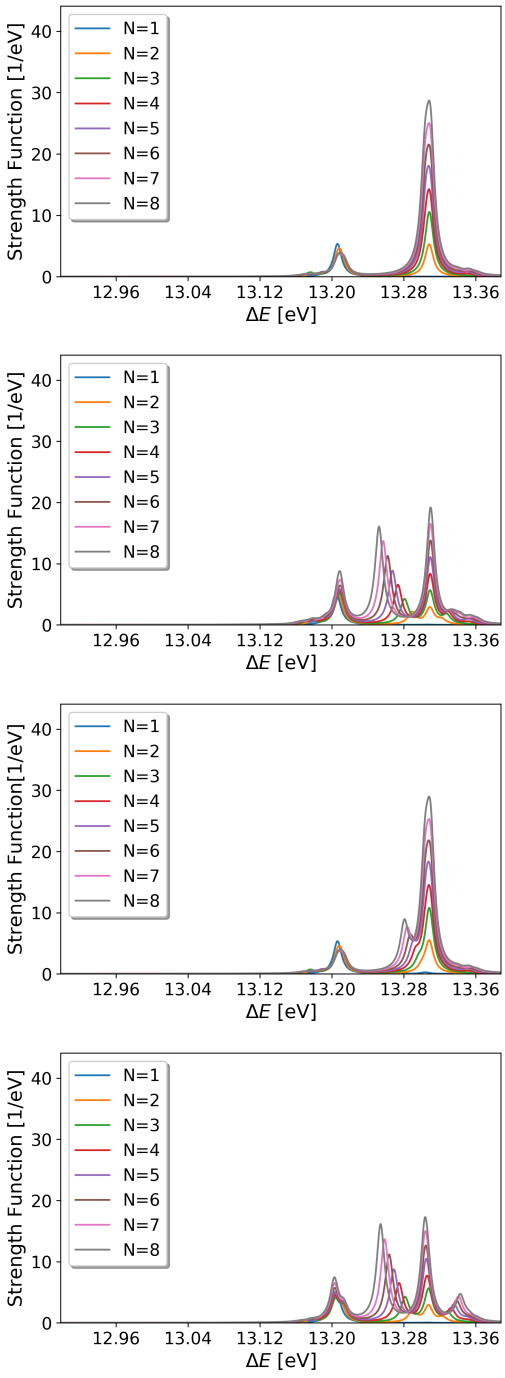

Figure S2: Nitrogen dimer chain of variable size $N \in \{1..9\}$ with one perturbed dimer. From top to bottom: $\boldsymbol{\lambda} = 0$, $\boldsymbol{\lambda} \parallel \mathbf{e}_x$, $\boldsymbol{\lambda} \parallel \mathbf{e}_y$ and $\boldsymbol{\lambda} \parallel \mathbf{e}_z$.

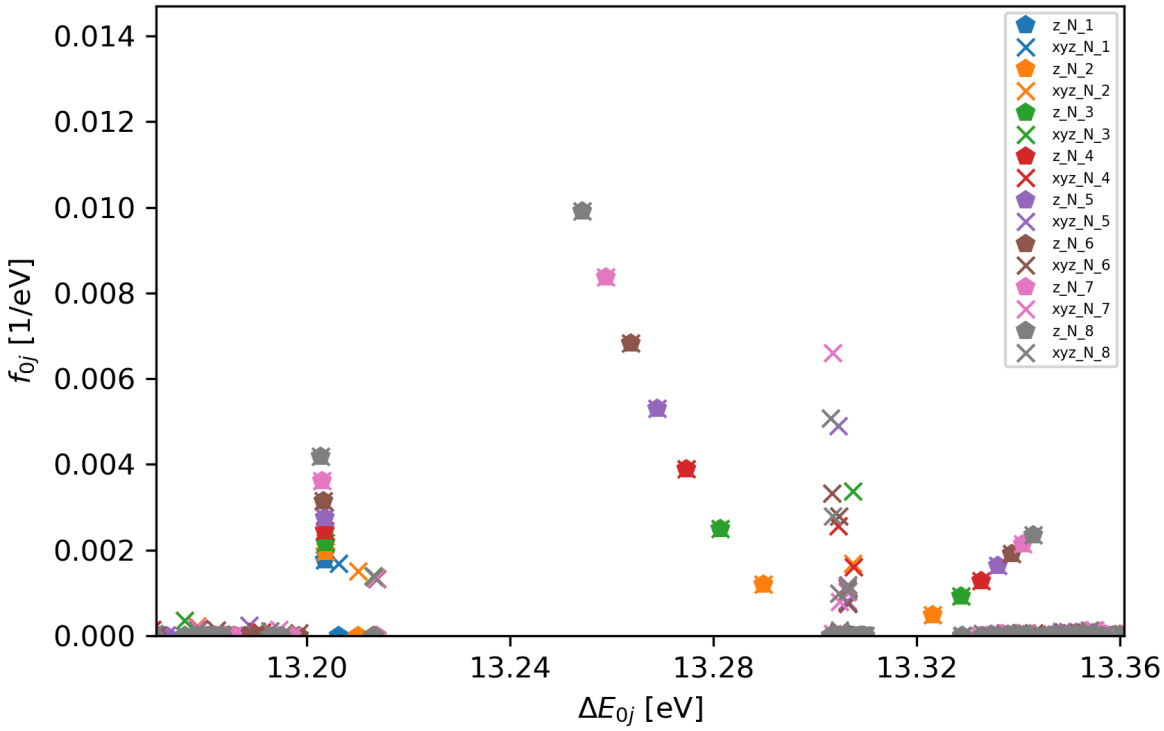

Figure S3: Oscillator strengths for perturbed dimer chain of variable size, with cavity oriented along z-axis in coupling regime I. Bold symbols indicate only contributions from transition dipolements along z whereas crosses account equally weighted for all three transition dipole moments along x, y, z. The later acts as a basis for the standard Lorentz-broadened spectra.

Local Properties

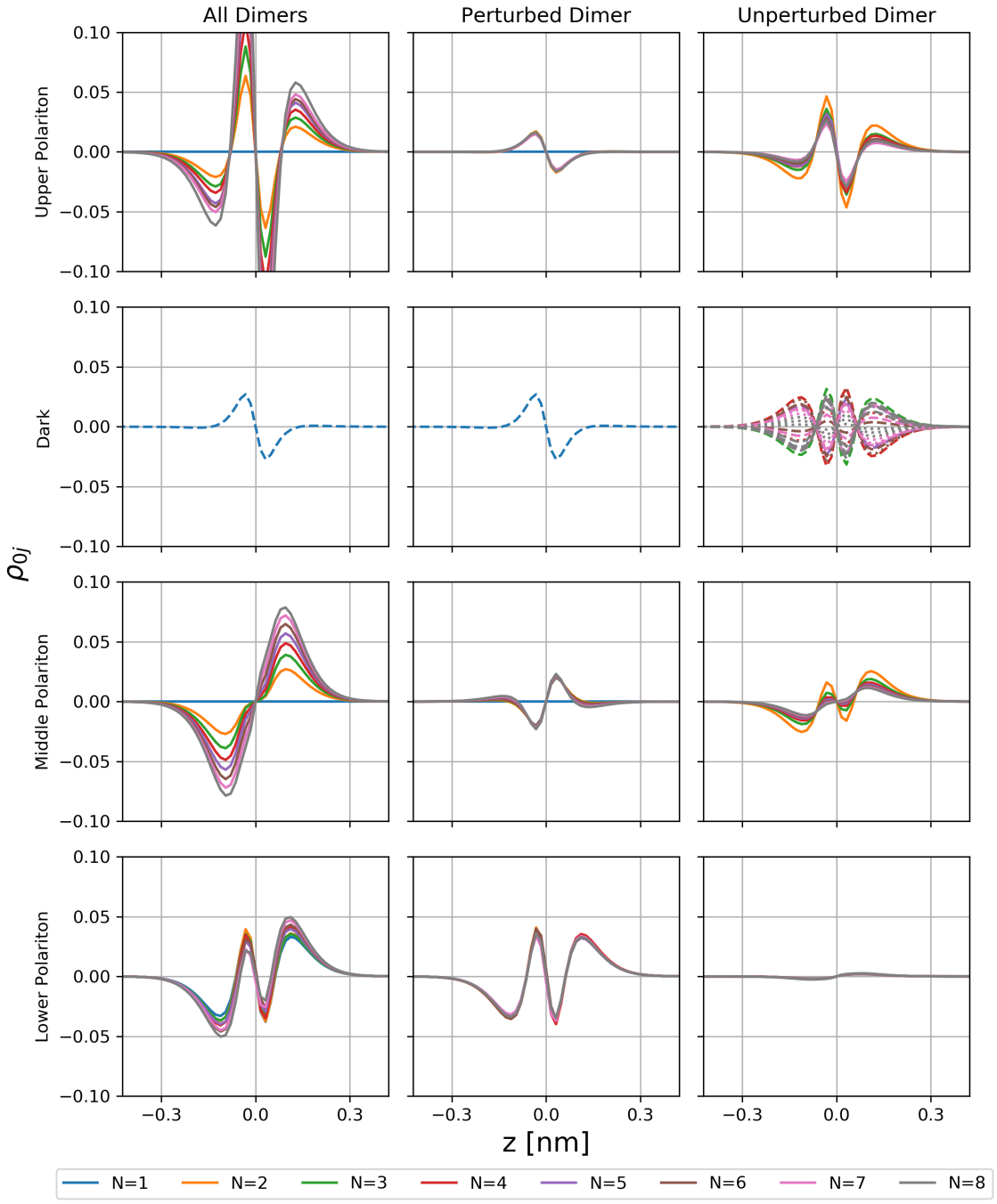

Figure S4: Globally (left column) and locally resolved transition densities projected onto the z-axis for different chain lengths N in coupling regime I. For each of the four energy windows (rows), integrated quantities are displayed, except for the dark states. The integration cleans the data and contributes only very little to the overall results.

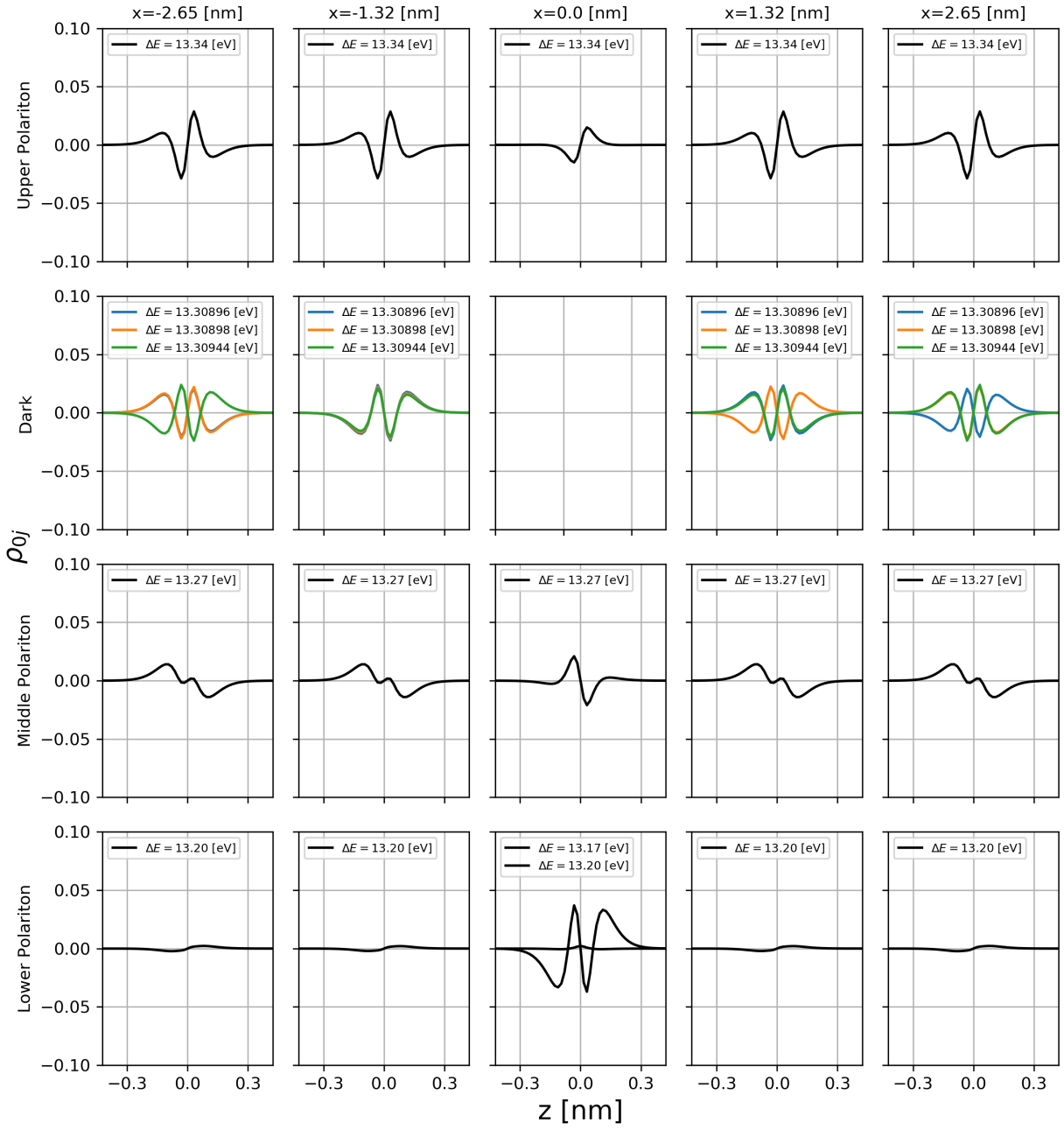

Figure S5: Locally resolved transition densities of each dimer projected onto the z-axis for $N = 5$ and coupling regime I. For each of the four energy windows (rows), integrated quantities are displayed, except for the three emerging dark states.

Simulation Results for Coupling Regime II ($\lambda = 0.005$)

Absorption Spectra for Cavity in Resonance with Unperturbed Dimers

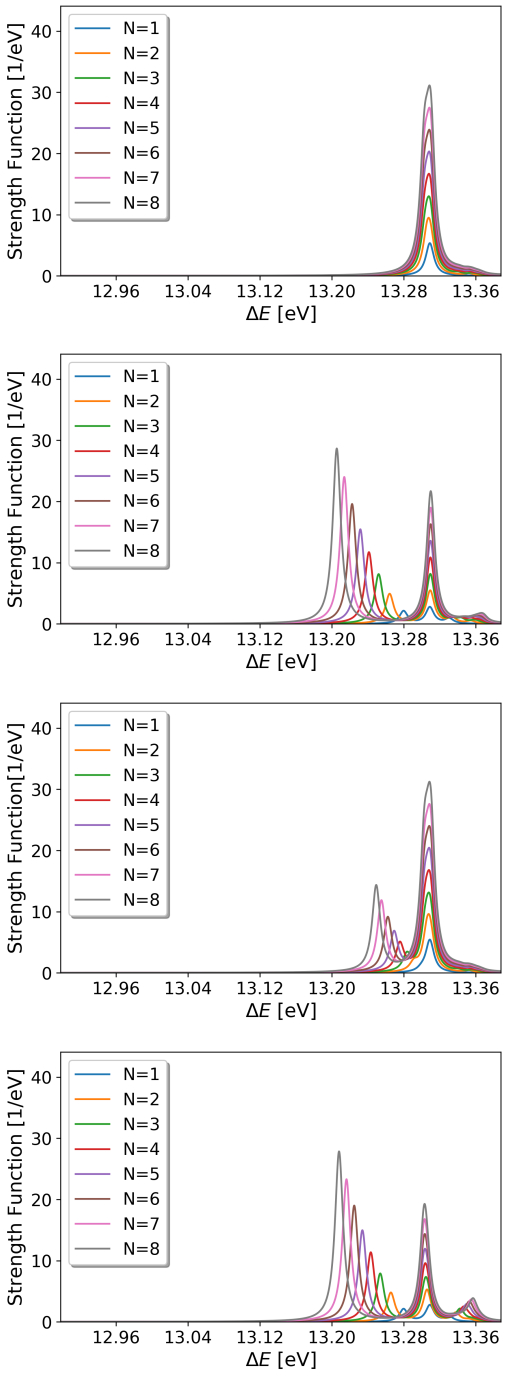

Figure S6: Nitrogen dimer chain of variable size $N \in \{1..9\}$ without perturbed dimer. From top to bottom: $\boldsymbol{\lambda} = 0$, $\boldsymbol{\lambda} \parallel \mathbf{e}_x$, $\boldsymbol{\lambda} \parallel \mathbf{e}_y$ and $\boldsymbol{\lambda} \parallel \mathbf{e}_z$.

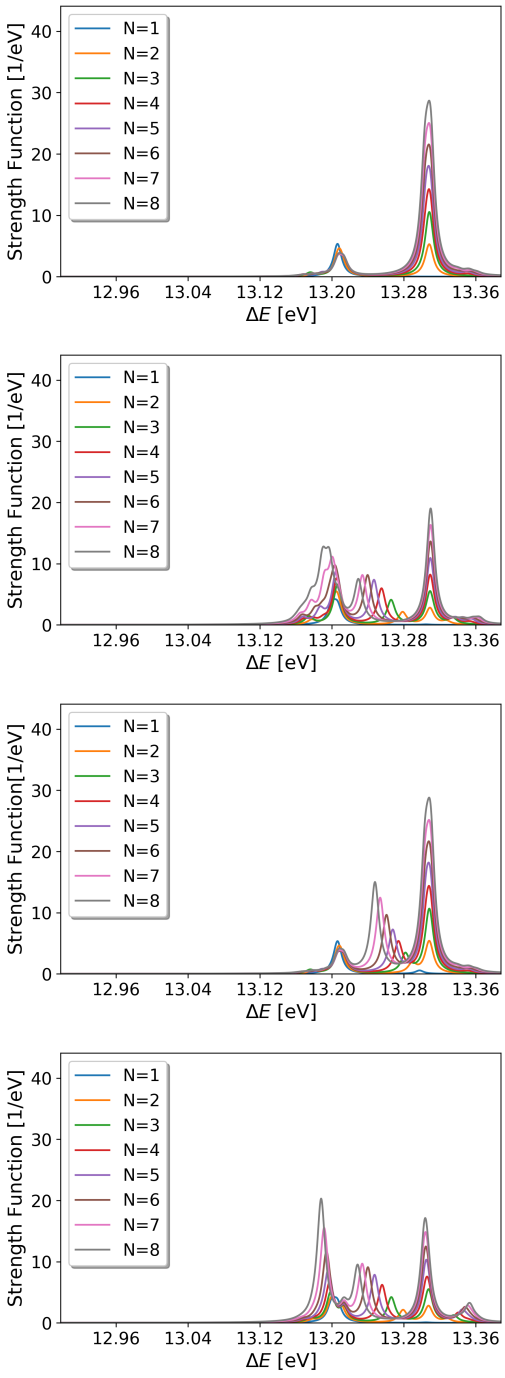

Figure S7: Nitrogen dimer chain of variable size $N \in \{1..9\}$ with one perturbed dimer. From top to bottom: $\boldsymbol{\lambda} = 0$, $\boldsymbol{\lambda} \parallel \mathbf{e}_x$, $\boldsymbol{\lambda} \parallel \mathbf{e}_y$ and $\boldsymbol{\lambda} \parallel \mathbf{e}_z$.

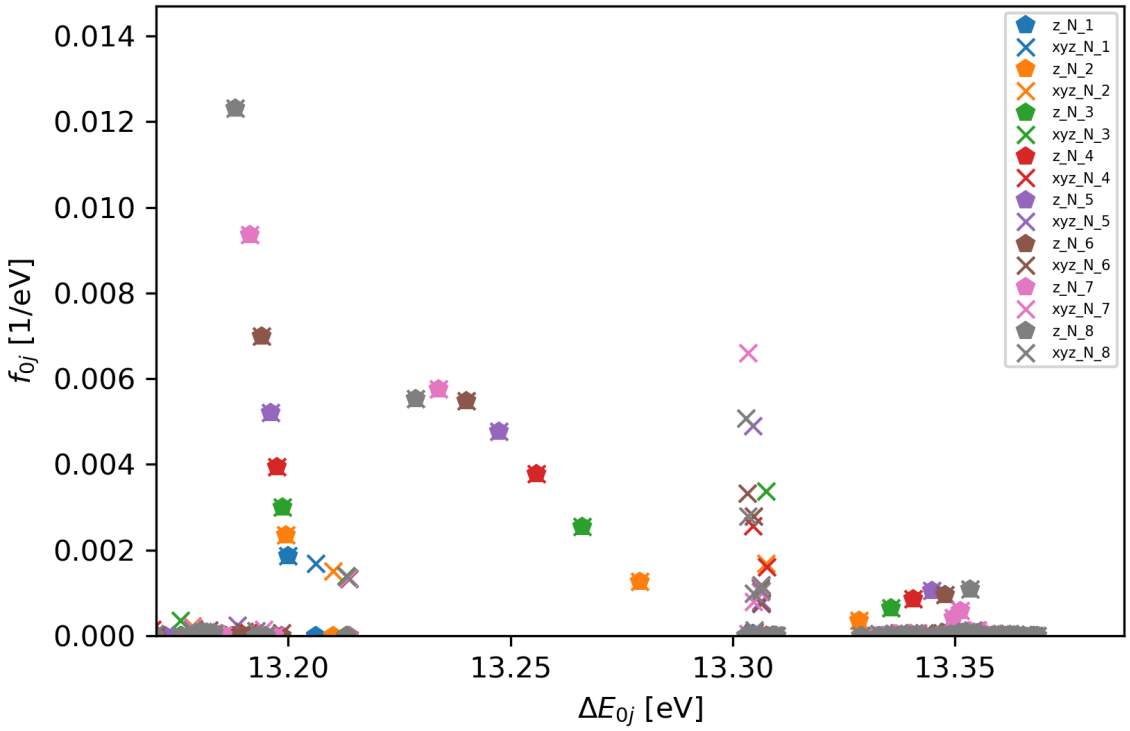

Figure S8: Oscillator strengths for perturbed dimer chain of variable size, with cavity oriented along z-axis in coupling regime II. Bold symbols indicate only contributions from transition dipolements along z whereas crosses account equally weighted for all three transition dipole moments along x, y, z. The later acts as a basis for the previously shown Lorentz-broadened spectra. Notice the splitting in the upper polaritonic branch for $N = 7$ (labeled z_N_7 in purple), which is caused by a sign change of the $N - 1$ unperturbed transition dipole moments. Whether or not real systems can be prepared to enter this novel regime, will be topic of future investigations.

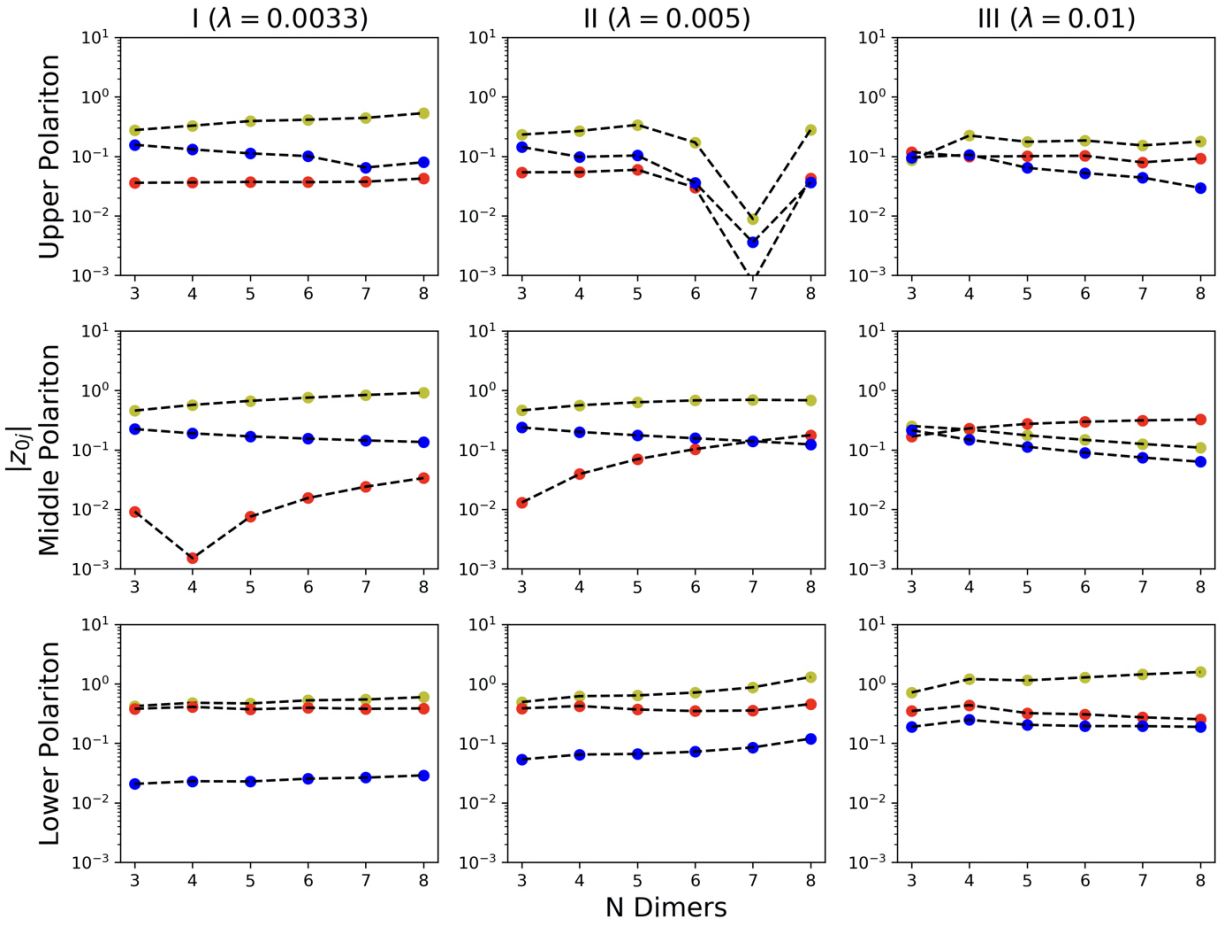

Figure S9: Global (yellow) and local transition dipole moment scaling with respect to different chain lengths for the perturbed (red) and unperturbed (blue) dimers. Special cases $N = \{1, 2\}$ are excluded for the sake of clarity (either does not include an unperturbed dimer or no dark states can form).

Mimic collectively induced modifications of the impurity with a suitable choice of λ

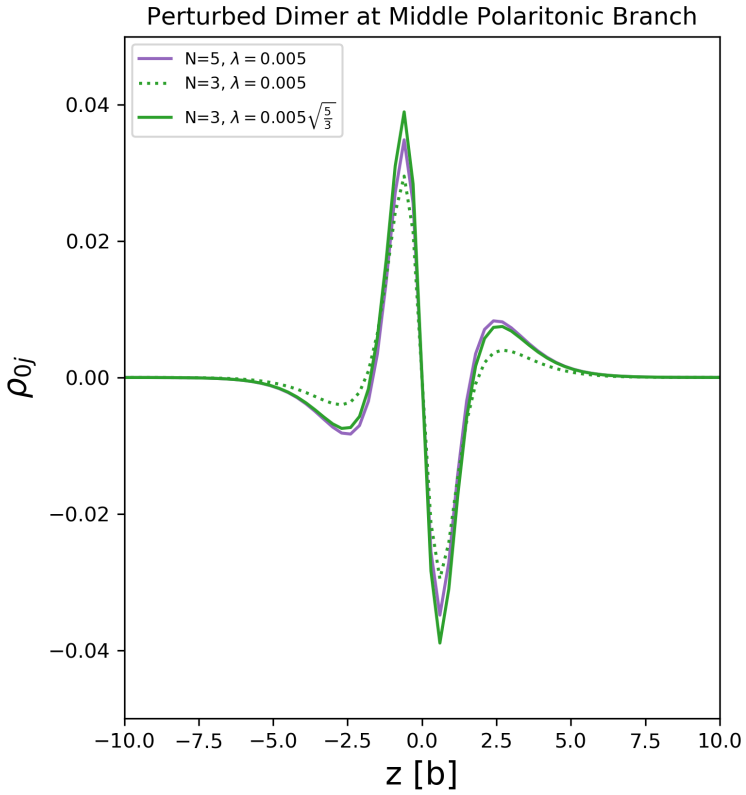

Figure S10: Local transition density for the perturbed dimer in the middle polaritonic branch for coupling regime II. The scaling up of λ for $N = 3$ allows to mimic locally imposed effects on the perturbed dimer, which arise from collective coupling in larger systems (here $N = 5$). This opens the door for efficient *ab initio* simulation methods in polaritonic chemistry.

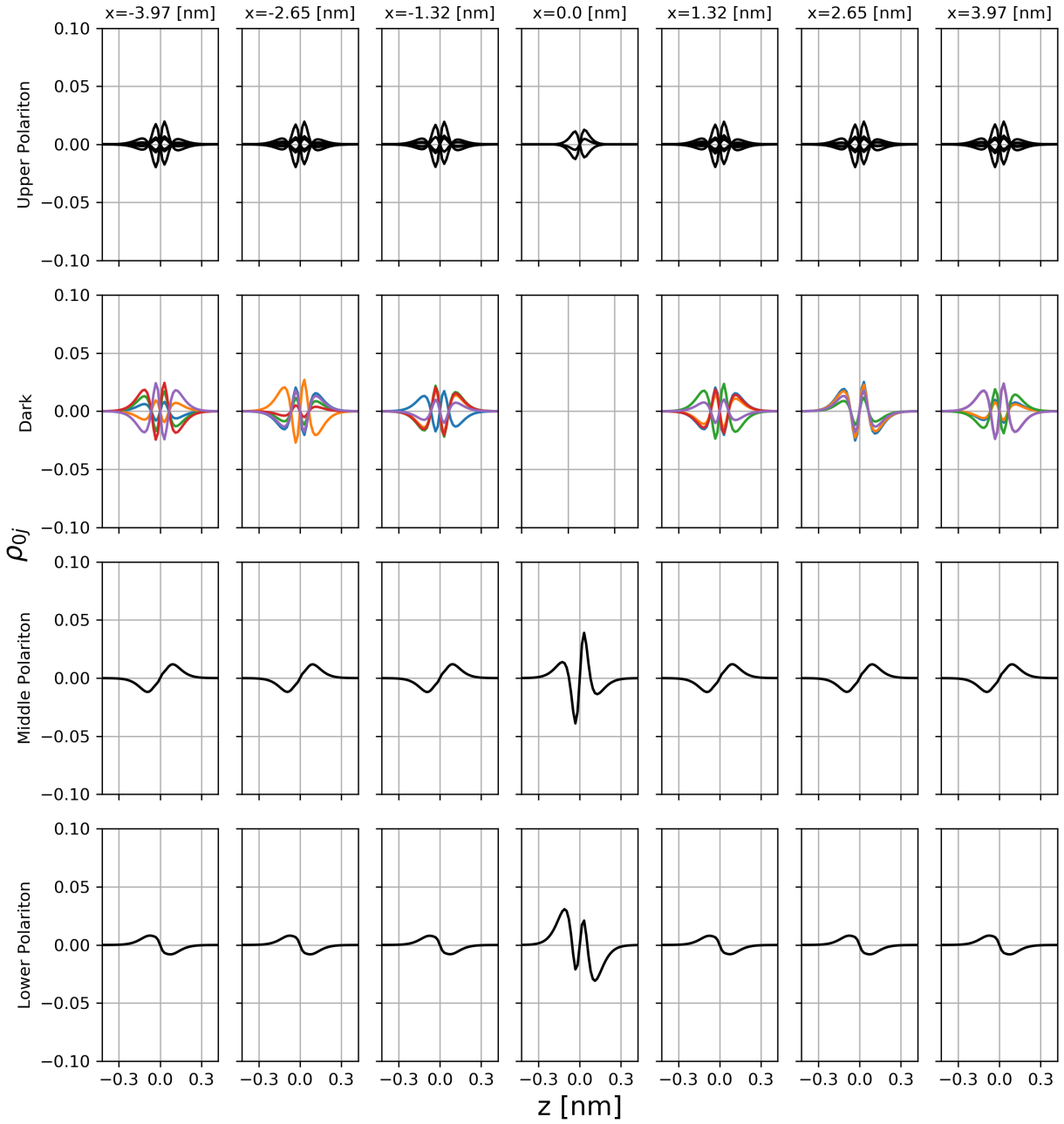

Figure S11: Locally resolved transition densities of each dimer projected onto the z-axis for $N = 7$ and coupling regime II. Cavity tuned to unperturbed frequency ω_u and $\lambda = 0.005$. For each of the four energy windows (rows), integrated quantities are displayed, except for the emerging dark states (in color). Notice that the different dark state patterns have significantly different local transition densities.

Absorption Spectra for Cavity in Resonance with Perturbation

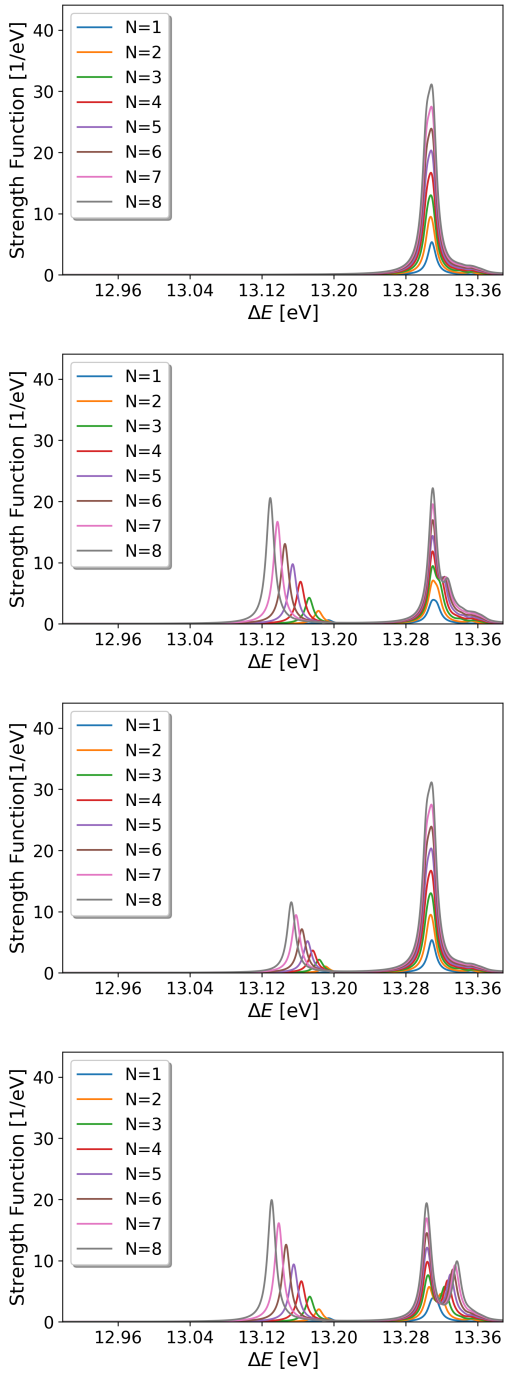

Figure S12: Nitrogen dimer chain of variable size $N \in \{1..9\}$ without perturbed dimer. Cavity tuned to perturbed frequency ω_p (!) and $\lambda = 0.005$. From top to bottom: $\boldsymbol{\lambda} = 0$, $\boldsymbol{\lambda} \parallel \mathbf{e}_x$, $\boldsymbol{\lambda} \parallel \mathbf{e}_y$ and $\boldsymbol{\lambda} \parallel \mathbf{e}_z$.

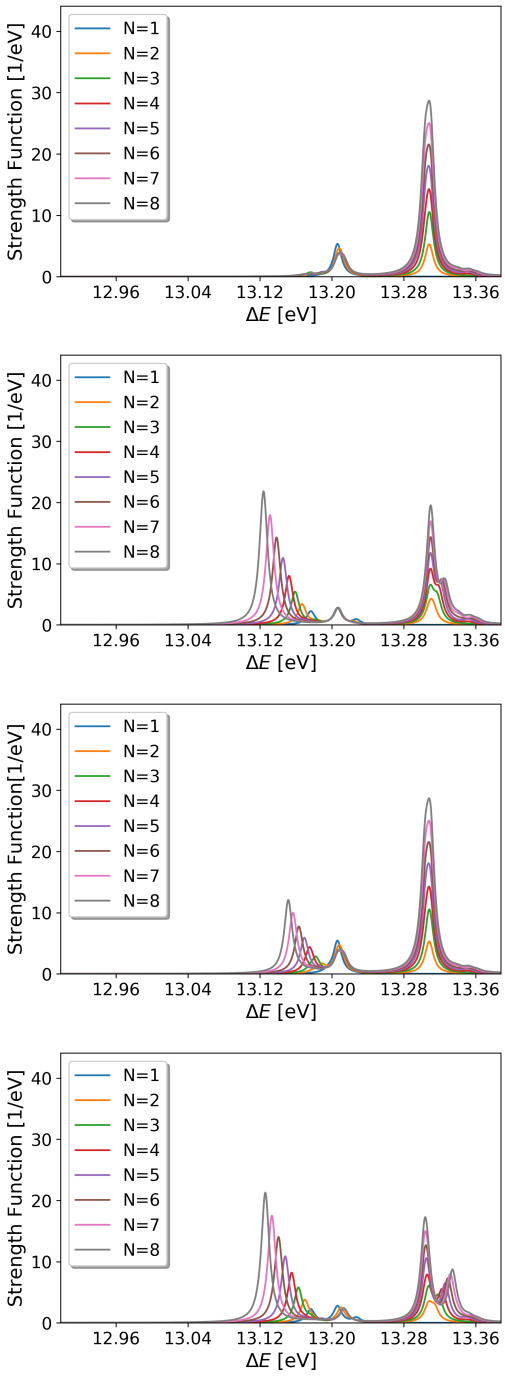

Figure S13: Nitrogen dimer chain of variable size $N \in \{1..9\}$ with one perturbed dimer. Cavity tuned to perturbed frequency ω_p (!) and $\lambda = 0.005$. From top to bottom: $\boldsymbol{\lambda} = 0$, $\boldsymbol{\lambda} \parallel \mathbf{e}_x$, $\boldsymbol{\lambda} \parallel \mathbf{e}_y$ and $\boldsymbol{\lambda} \parallel \mathbf{e}_z$.

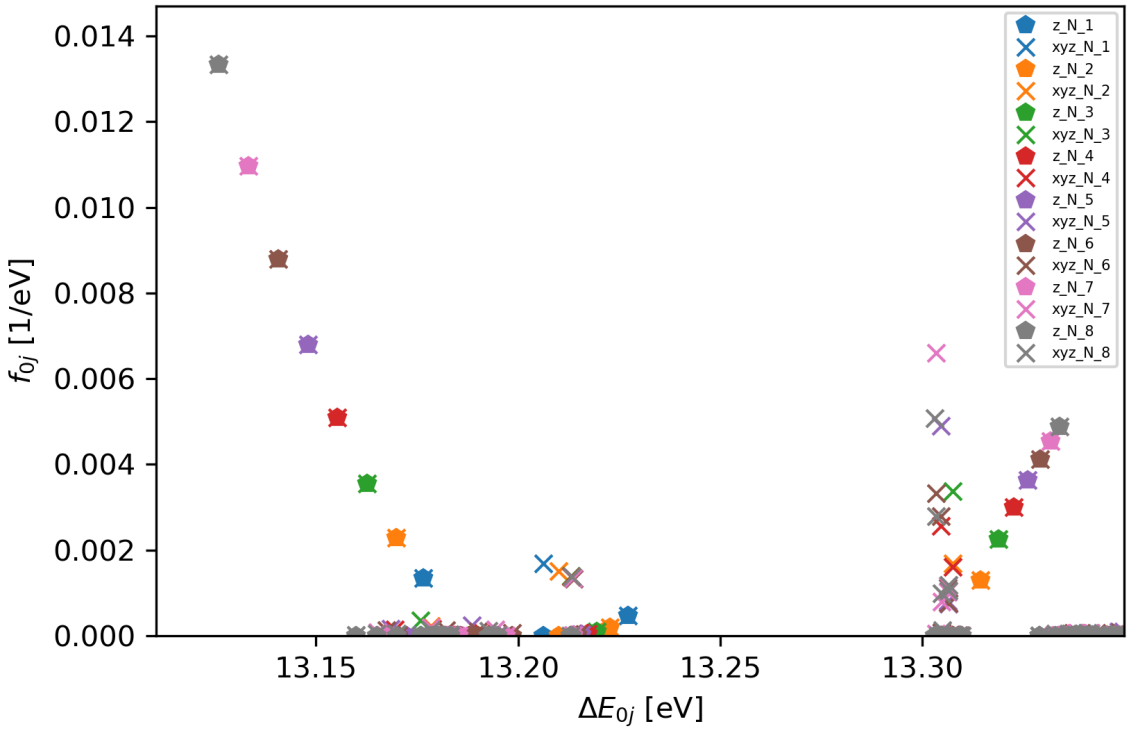

Figure S14: Oscillator strengths for perturbed dimer chain of variable size, with cavity oriented along z-axis in coupling regime II. Cavity tuned to perturbed frequency ω_p (!) and $\lambda = 0.005$. Bold symbols indicate only contributions from transition dipolements along z whereas crosses account equally weighted for all three transition dipole moments along x, y, z. The later acts as a basis for the previously shown Lorentz-broadened spectra.

Local Properties

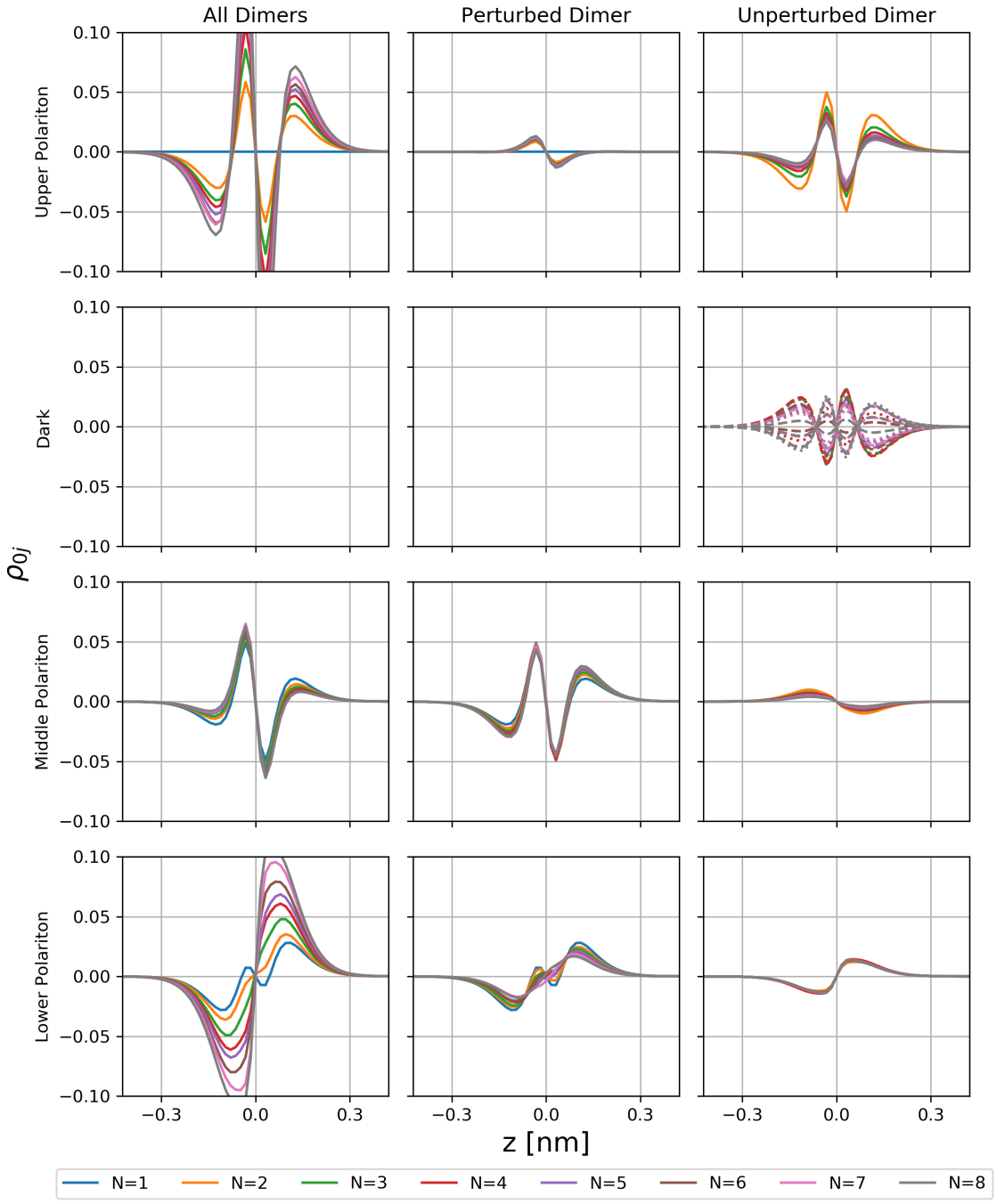

Figure S15: Globally (left column) and locally resolved transition densities projected onto the z-axis for different chain lengths N in coupling regime II. Cavity tuned to perturbed frequency ω_p (!) and $\lambda = 0.005$. For each of the four energy windows (rows), integrated quantities are displayed, except for the dark states. The integration cleans the data and contributes only very little to the overall results.

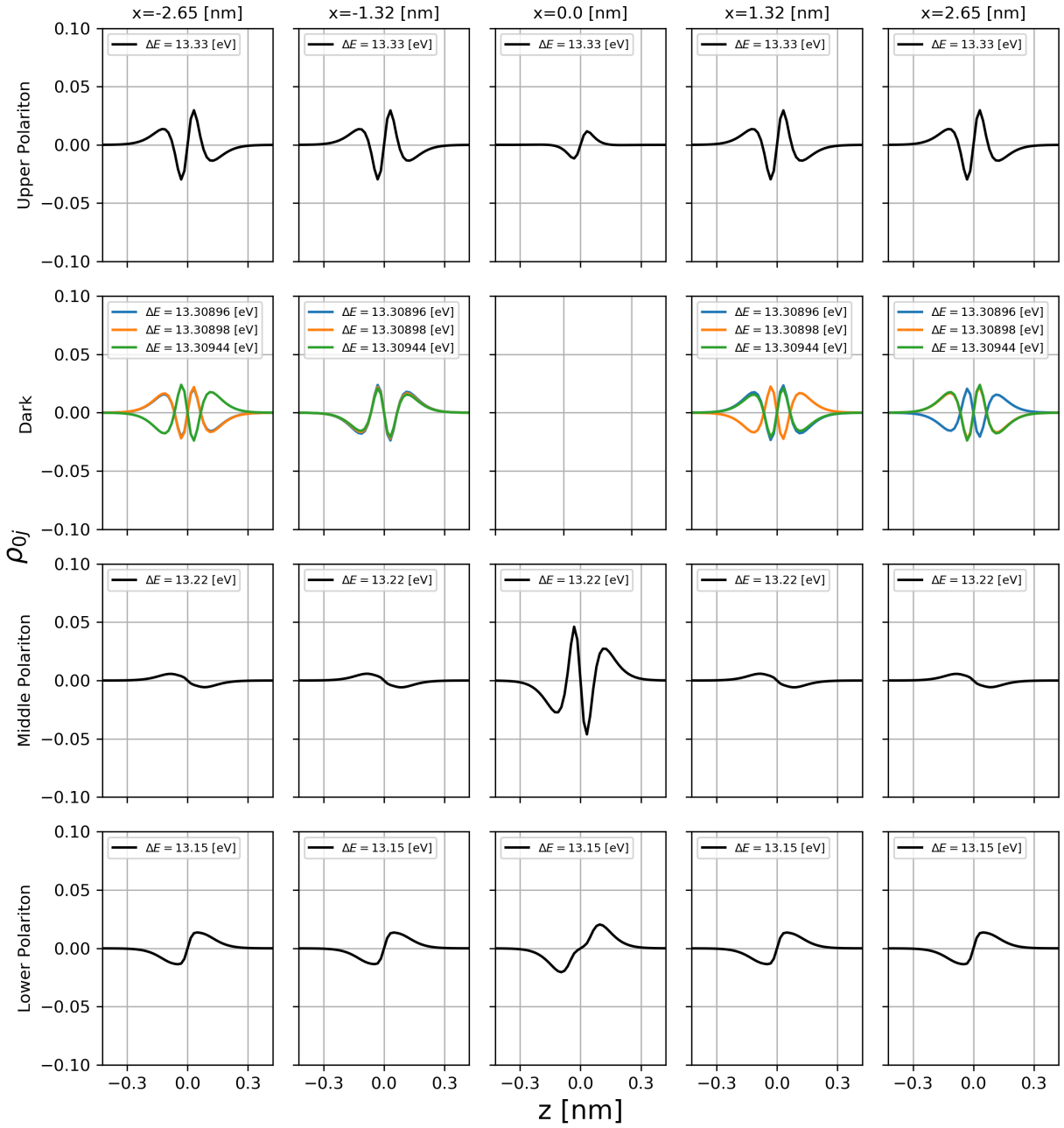

Figure S16: Locally resolved transition densities of each dimer projected onto the z-axis for $N = 5$ and coupling regime II. Cavity tuned to perturbed frequency ω_p (!) and $\lambda = 0.005$. For each of the four energy windows (rows), integrated quantities are displayed, except for the three emerging dark states.

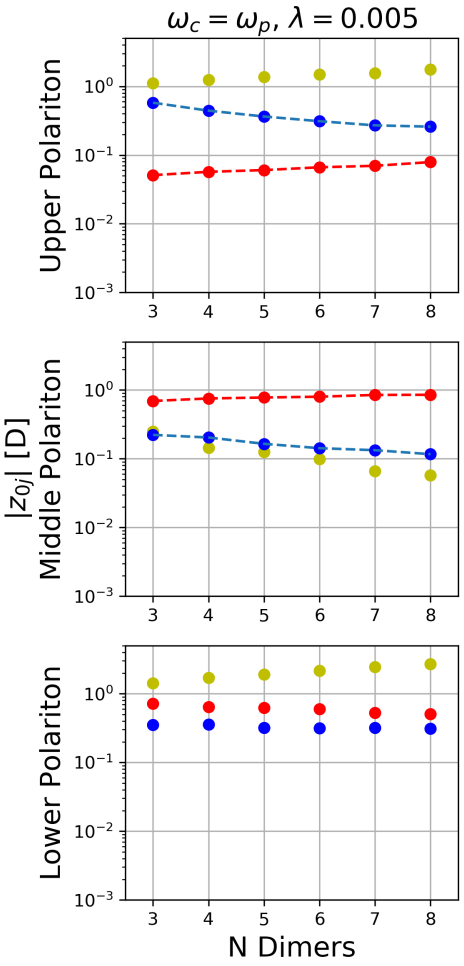

Figure S17: Collective (yellow) and local transition dipole moment scaling with respect to different chain lengths N for the perturbed (red) and unperturbed (blue) dimers in coupling regime II. The cavity is tuned on ω_p. Special cases $N = \{1, 2\}$ are excluded for the sake of clarity (either does not include an unperturbed dimer or no dark states can form). Opposing local scaling behaviour is indicated by blue and red lines. In contrast to the cavity tuned on the unperturbed dimers ω_p, we observe here opposite scaling behaviour also in the upper polaritonic branch and not only for the middle polaritonic branch.

Simulation Results for Coupling Regime III ($\lambda = 0.01$)

Absorption Spectra for Cavity in Resonance with Unperturbed Dimers

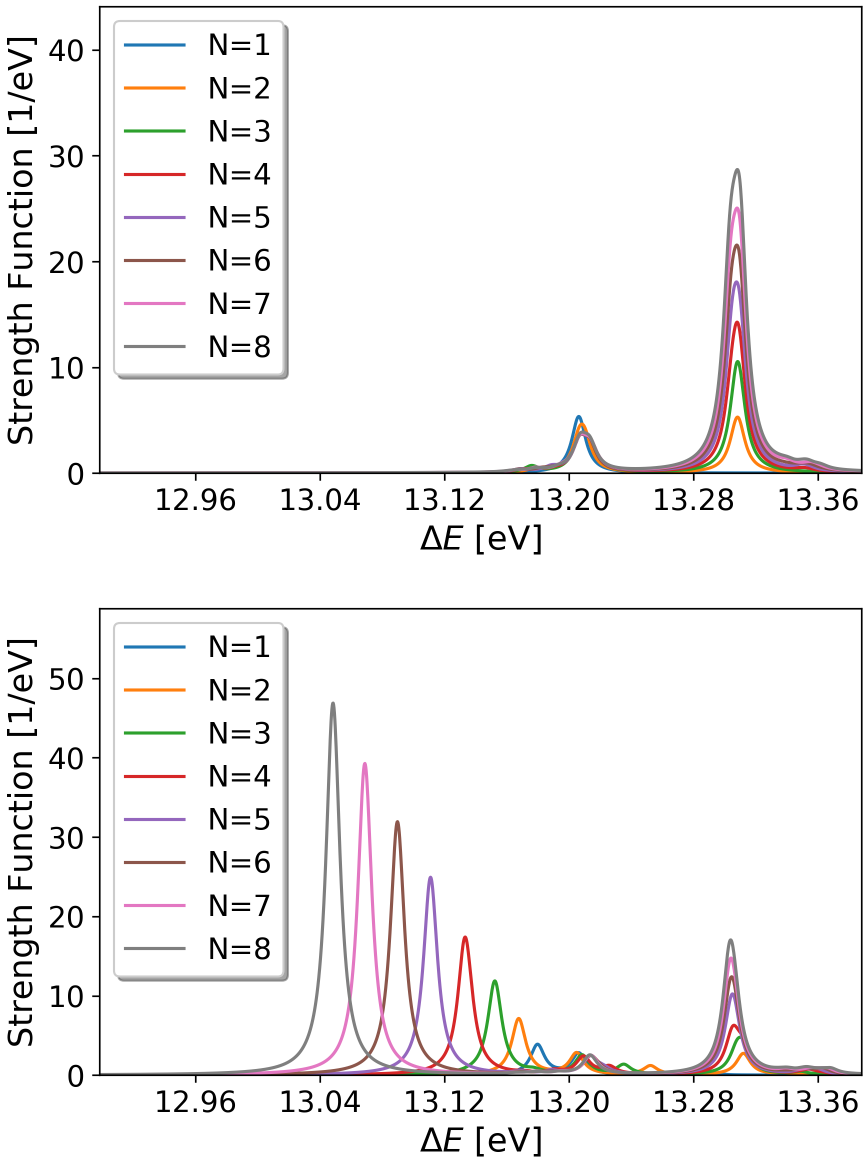

Figure S18: Nitrogen dimer chain of variable size $N \in \{1..9\}$ with one perturbed dimer. From top to bottom: $\boldsymbol{\lambda} = 0$ and $\boldsymbol{\lambda} \parallel \mathbf{e}_z$.

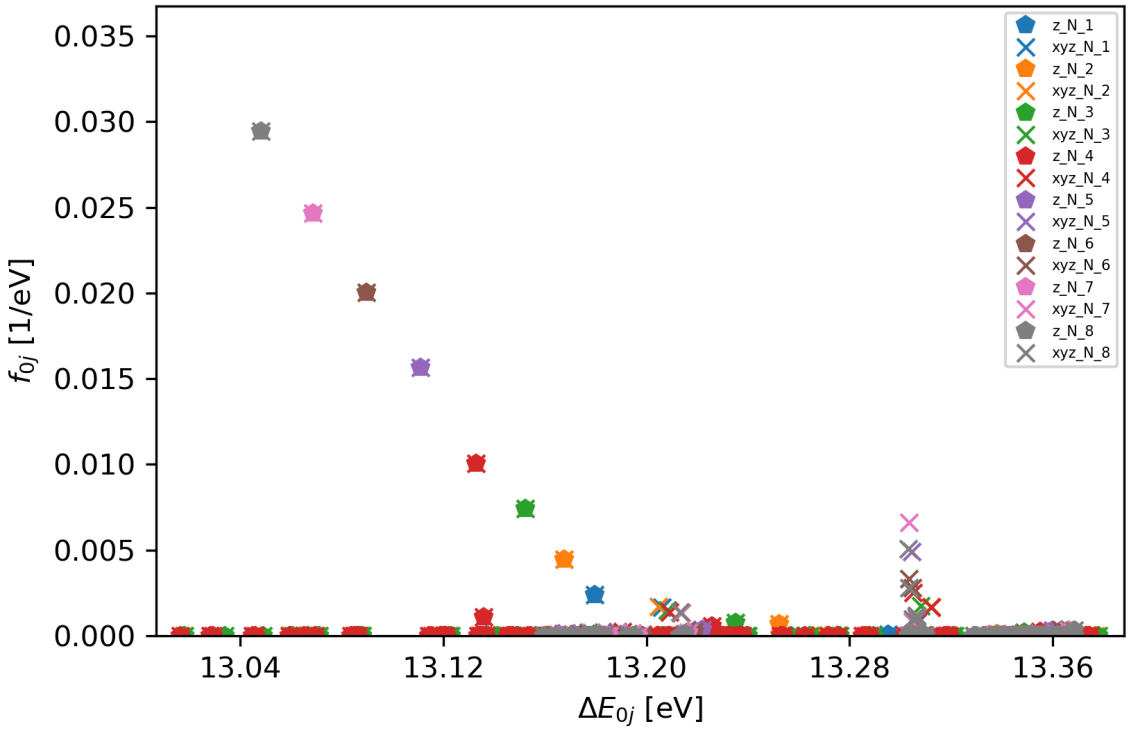

Figure S19: Oscillator strengths for perturbed dimer chain of variable size, with cavity oriented along z-axis in coupling regime III. Bold symbols indicate only contributions from transition dipolements along z whereas crosses account equally weighted for all three transition dipole moments along x, y, z. The later acts as a basis for the previously shown Lorentz-broadened spectra.

Local Properties

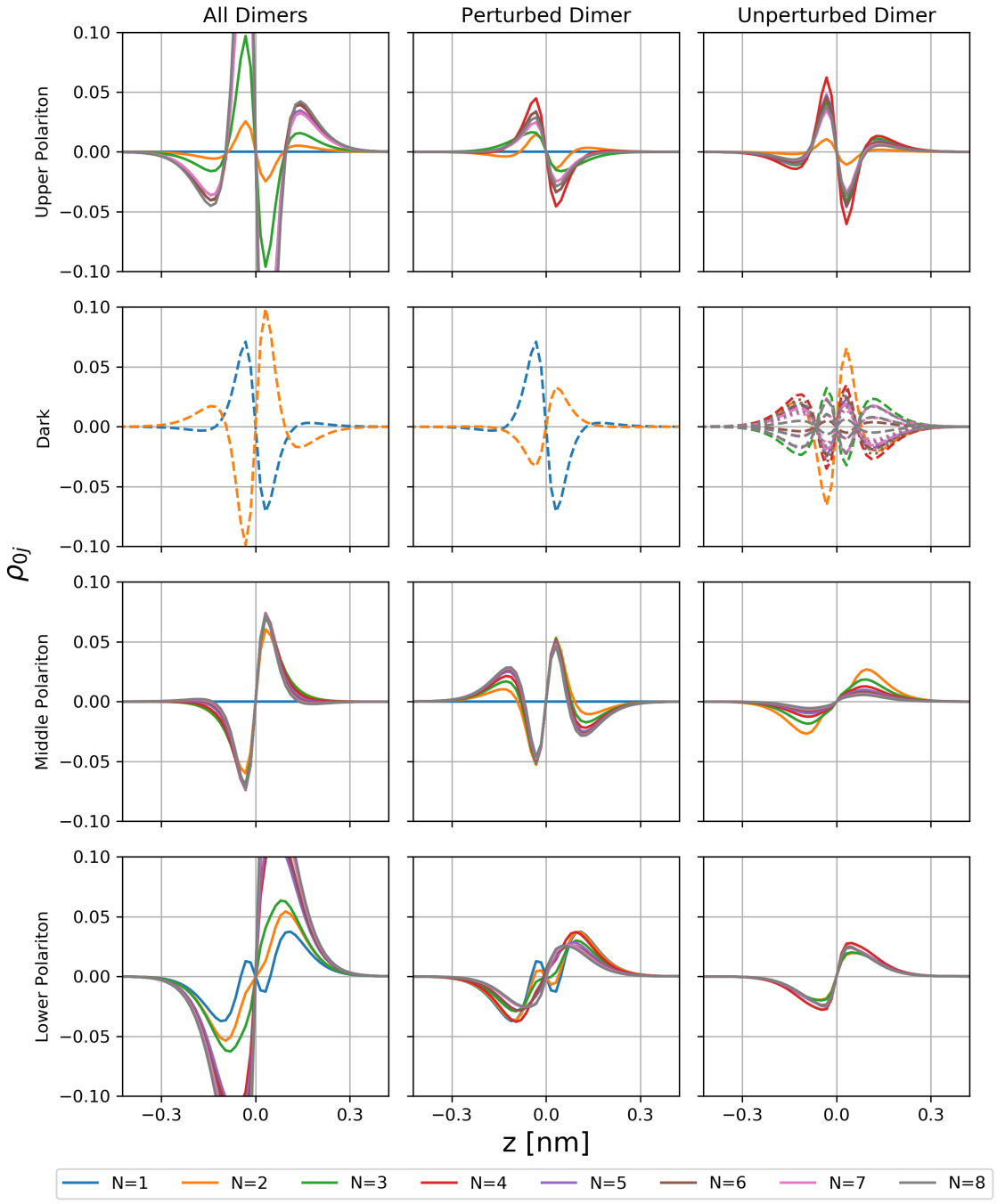

Figure S20: Globally (left column) and locally resolved transition densities projected onto the z-axis for different chain lengths N in coupling regime III. For each of the four energy windows (rows), integrated quantities are displayed, except for the dark states. The integration cleans the data and contributes only very little to the overall results.

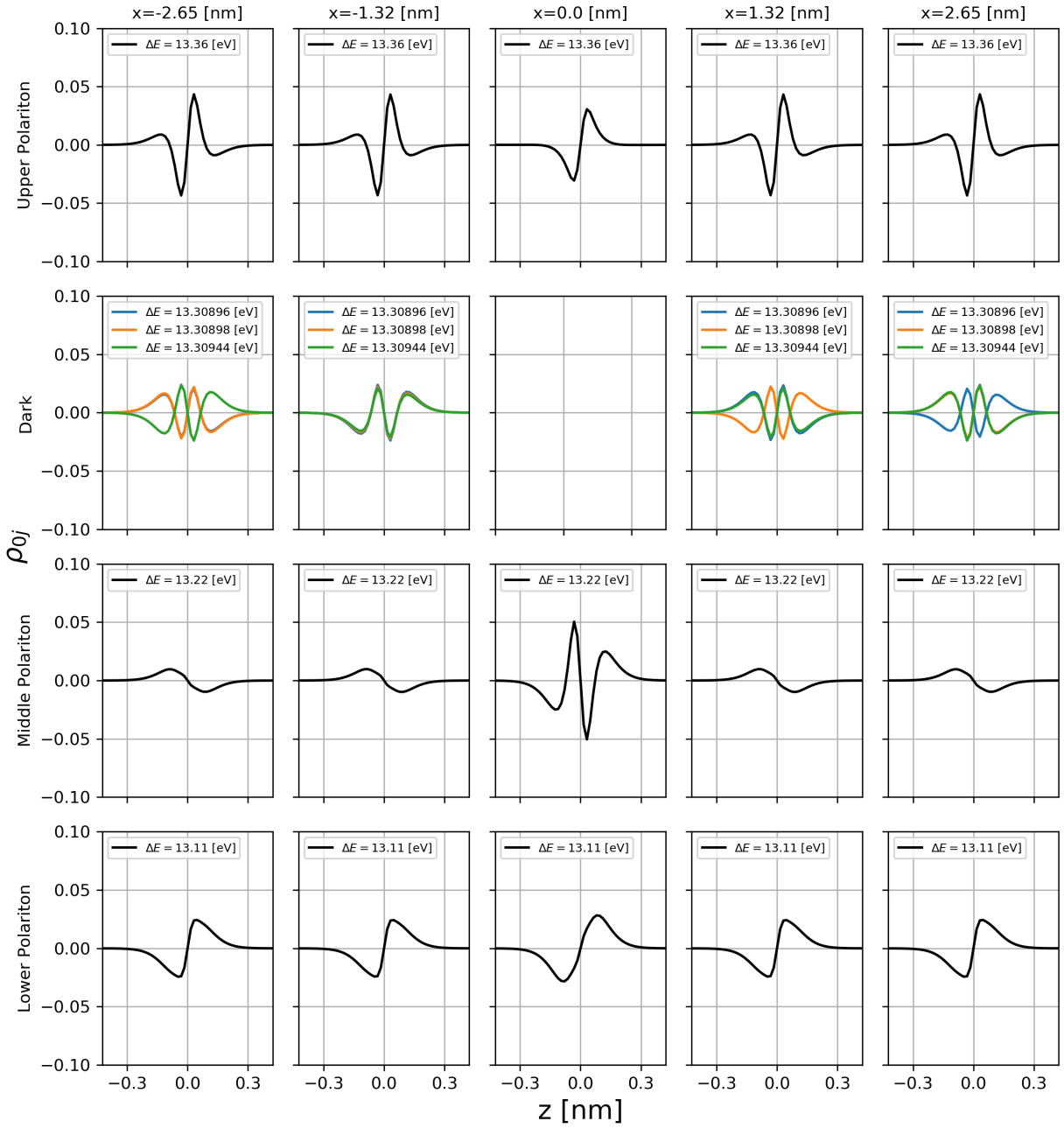

Figure S21: Locally resolved transition densities of each dimer projected onto the z-axis for $N = 5$ and coupling regime III. For each of the four energy windows (rows), integrated quantities are displayed, except for the three emerging dark states.

References

(1) Tancogne-Dejean, N.; Oliveira, M. J.; Andrade, X.; Appel, H.; Borca, C. H.; Le Breton, G.; Buchholz, F.; Castro, A.; Corni, S.; Correa, A. A. et al. Octopus, a Computational Framework for Exploring Light-Driven Phenomena and Quantum Dynamics in Extended and Finite Systems. *J. Chem. Phys.* **2020**, *152*, 124119.

(2) Flick, J.; Welakuh, D. M.; Ruggenthaler, M.; Appel, H.; Rubio, A. Light–Matter Response in Nonrelativistic Quantum Electrodynamics. *ACS Photonics* **2019**, *6*, 2757–2778.

(3) Krieger, J.; Li, Y.; Iafrate, G. Derivation and Application of an Accurate Kohn-Sham Potential with Integer Discontinuity. *Phys. Lett. A* **1990**, *146*, 256–260.

(4) Krieger, J.; Li, Y.; Iafrate, G. Construction and Application of an Accurate Local Spin-Polarized Kohn-Sham Potential with Integer Discontinuity: Exchange-Only Theory. *Phys. Rev. A* **1992**, *45*, 101.

(5) Krieger, J.; Li, Y.; Iafrate, G. Systematic Approximations to the Optimized Effective Potential: Application to Orbital-Density-Functional Theory. *Phys. Rev. A* **1992**, *46*, 5453.

(6) Li, Y.; Ullrich, C. Time-Dependent Transition Density Matrix. *Chem. Phys.* **2011**, *391*, 157–163.